Detailed Computational Modeling Methods

Two Markov models, one representing hERG 1a/1b and another representing hERG 1a, were constructed using a previous model for I_{Kr} as a template[1]. Simulations for model validation reproduced the experimental protocols, including temperature (exception: the E-4031 dose response curve was measured at room temperature, but was simulated without adjusting the models which were validated at near-physiological temperature). Matlab and the ode23s integrator (absolute and relative error tolerance set to 10^{-6}) were used to compute these simulations using a Windows XP desktop computer with a Pentium 4 processor. Parameters were chosen using the interior-reflective Newton method[2] and a least squares objective function to match action potential clamp data for hERG 1a/1b. This was followed by manual refinements to improve correspondence of the models with all of the other data for hERG 1a/1b and to determine the hERG 1a parameters. Equations for the hERG models are given in this online supplement. The hERG models were incorporated into the Fink modified[3] ten Tusscher action potential model[4] in exchange for the native I_{Kr}. Action potential simulations were computed using Rush and Larson integration[5] for the cell model (fixed time step = 0.01 ms) and the CVODE[6] integrator for the hERG models (several time steps per 0.01 ms). They were implemented in C++ and run on Linux cluster nodes. All action potential results show the 1000th beat at 1 Hz pacing.

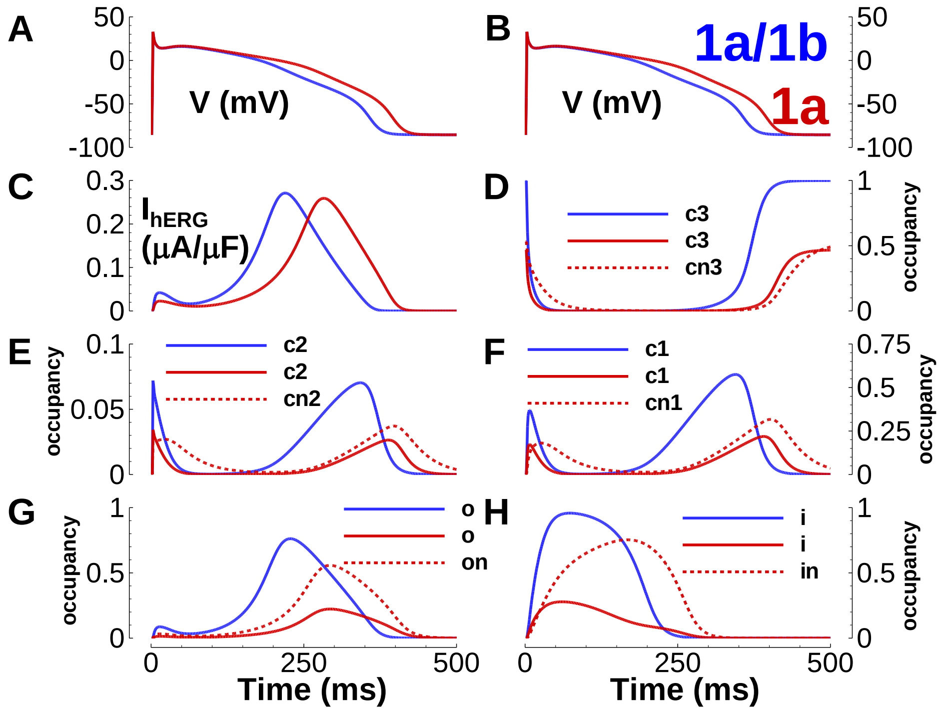

Online Figure I. *Comparison of hERG 1a/1b (blue) and hERG 1a (red) in the action potential without E-4031*. Shown are results from the 1000th paced beat at 1 Hz for the Fink modified[3] ten Tusscher action potential model[4]. A&B) Action potentials. C) hERG 1a/1b (blue) hERG 1a/1b (blue) and hERG 1a (solid red for normal mode, and dashed red for N-mode). E-4031-blocked state occupancies are zero for hERG 1a/1b and for hERG 1a (not shown) since the drug is not applied in this simulation. APD_{90} (measure of the time elapsed between activation and 90% repolarization) for hERG 1a is 376 ms. This is 38 ms longer than APD_{90} for hERG 1a/1b. The hERG 1a versus hERG 1a/1b prolongation is 30 ms when our models are incorporated into the Priebe and Beuckelmann action potential model[7] (not shown). Prolongation occurs because N-mode occupancy results in slower activation, and slower closed-state inactivation. N-mode activation is movement from *cn3*, to *cn2*, to *cn1*. This movement is slow compared with *c3*, to *c2*, to *c1* movement in the normal mode because N-mode activation/deactivation rates are reduced to 0.35 times the normal mode values. A comparison of early growth and decay for solid versus dashed red lines in panels D-F illustrates this. Closed-state inactivation in the N-mode, which is movement from *cn1* to *in*, is slower than the corresponding normal mode movement from *c1* to *i*. This is because the N-mode transition rate $\alpha n2$ is reduced to 0.35 times the corresponding normal mode transition rate $\alpha 2$. Thus, recovery current through the open state arrives after a delay in N-mode compared to normal mode. Panels F and H illustrate. In panel F, early *cn1* decay is slower than *c1* decay. In panel H, decay from normal mode state *i* begins at t = 60 ms while N-mode decay from state *in* does not begin until 108 ms later, when *cn1* finally finishes emptying into *in*.

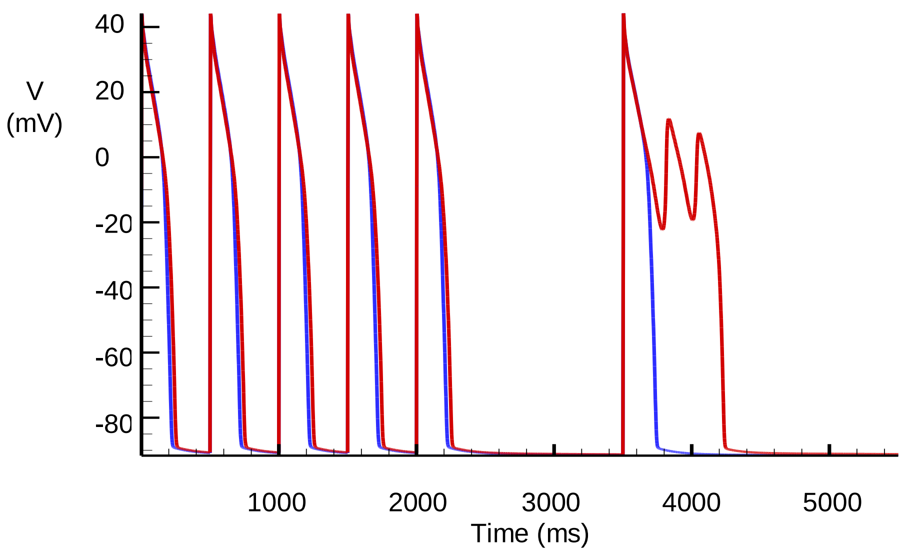

Online Figure II. *Pause-induced early afterdepolarizations for hERG 1a (red), but not for hERG 1a/1b (blue) in the presence of E-4031.* To test for susceptibility to early afterdepolarizations we used the Luo-Rudy midmyocardial ventricular action potential model[8]. Unlike the human-based Fink modified ten Tusscher model and the Priebe and Beuckelmann model used elsewhere in this study, the guinea pig-based Luo-Rudy model has features that enable the reliable demonstration of early afterdepolarizations under appropriate conditions.[9, 10] This figure shows the Luo-Rudy model paced for 40 beats at a cycle length of 500 ms with hERG 1a or hERG 1a/1b in place of the native I_{Kr}. Following these 40 beats (of which the last five are shown), a 1500 ms pause preceded an additional single paced beat. [E-4031] was set to 55 nM, the minimum concentration needed to cause an early afterdepolarization. The formation of early afterdepolarizations for hERG 1a but not for hERG 1a/1b demonstrates a connection between the altered channel kinetics of hERG 1a and the clinical appearance of *torsades de pointes* arrhythmia in the presence of hERG blocking drugs following a pause[11].

Model Equations.

hERG 1a/1b model transition rates (ms^{-1})

$$\alpha = 0.03552 * \exp\left[1.812 * \frac{VF}{RT}\right]$$
$$\beta = 1.807e-3 * \exp\left[-1.913 * \frac{VF}{RT}\right]$$
$$\alpha 1 = 4.340$$
$$\beta 1 = 0.5409$$
$$\alpha 2 = 0.02620 * \exp\left[1.241 * \frac{VF}{RT}\right]$$
$$\beta 2 = 3.300e-3 * \exp\left[-0.9571 * \frac{VF}{RT}\right]$$
$$\alpha i = 0.1139 * \exp\left[-0.4898 * \frac{VF}{RT}\right] * \frac{4.5}{\left[K^+\right]_o}$$
$$\beta i = 0.1254 * \exp\left[0.3781 * \frac{VF}{RT}\right] * \left(\frac{4.5}{\left[K^+\right]_o}\right)^3$$
$$\mu = \frac{\alpha i * \beta 2}{\beta i}$$

$ON = [E4031] * 2.0e3$, with [E-4031] in mol/L
$OFF = 5.0e-6$

10 coupled ordinary differential equations

$$\frac{dc3}{dt} = c2 * \beta - c3 * \alpha$$
$$\frac{dc2}{dt} = c3 * \alpha + c1 * \beta 1 - c2 * (\beta + \alpha 1)$$
$$\frac{dc1}{dt} = c2 * \alpha 1 + o * \beta 2 + i * \mu - c1 * (\beta 1 + 2 * \alpha 2)$$
$$\frac{do}{dt} = c1 * \alpha 2 + i * \alpha i + b * OFF - o * (\beta 2 + \beta i + ON)$$
$$\frac{di}{dt} = c1 * \alpha 2 + o * \beta i - i * (\mu + \alpha i)$$
$$\frac{dcb3}{dt} = cb2 * \beta - cb3 * \alpha$$

$$\frac{dcb2}{dt} = cb3*\alpha + cb1*\beta 1 - cb2*(\beta + \alpha 1)$$
$$\frac{dcb1}{dt} = cb2*\alpha 1 + b*\beta 2 + ib*\mu - cb1*(\beta 1 + 2*\alpha 2)$$
$$\frac{db}{dt} = cb1*\alpha 2 + ib*\alpha i + o*ON - b*(\beta 2 + \beta i + OFF)$$
$$\frac{dib}{dt} = cb1*\alpha 2 + b*\beta i - ib*(\mu + \alpha i)$$

Initial Conditions

$$c3 = 1$$
$$c2 = c1 = o = i = cb3 = cb2 = cb1 = b = ib = 0$$

Calculation of Current

$\overline{G}_{hERG}$ = 0.0048 mS, Fink modified[3], ten Tusscher[4]

$\overline{G}_{hERG}$ = 0.015 mS, Priebe and Buekelmann[7]

$\overline{G}_{hERG}$ = 0.02614 mS, Luo and Rudy[8]

$$E_K = \frac{RT}{F}\ln\left([K^+]_o / [K^+]_i\right)$$
$$I_{hERG,1a/1b} = \overline{G}_{hERG} * \sqrt{[K^+]_o / 5.4} * o * (V - E_K)$$

hERG 1a model transition rates (ms^{-1})

$$\alpha = 0.03552 * \exp\left[1.812 * \frac{VF}{RT}\right]$$
$$\beta = 1.807e-3 * \exp\left[-1.913 * \frac{VF}{RT}\right]$$
$$\alpha 1 = 4.340$$
$$\beta 1 = 0.5409$$
$$\alpha 2 = 0.02620 * \exp\left[1.241 * \frac{VF}{RT}\right]$$
$$\beta 2 = 3.300e-3 * \exp\left[-0.9571 * \frac{VF}{RT}\right]$$

$$\alpha i = 0.1139 * \exp\left[-0.4898 * \frac{VF}{RT}\right] * \frac{4.5}{\left[K^+\right]_o}$$

$$\beta i = 0.1254 * \exp\left[0.3781 * \frac{VF}{RT}\right] * \left(\frac{4.5}{\left[K^+\right]_o}\right)^3$$

$$\mu = \frac{\alpha i * \beta 2}{\beta i}$$

$$\alpha n = 0.35 * \alpha$$

$$\beta n = 0.35 * \beta$$

$$\alpha n1 = 0.35 * \alpha 1$$

$$\beta n1 = 0.35 * \beta 1$$

$$\alpha n2 = 0.35 * \alpha 2$$

$$\beta n2 = 0.35 * \beta 2$$

$$\alpha ni = 0.4 * \alpha i$$

$$\beta ni = 1.2 * \beta i$$

$$\mu n = \frac{\alpha ni * \beta n2}{\beta ni}$$

$ON = [E4031] * 2.0e3$, with [E-4031] in mol/L

$$OFF = 5.0e-6$$

$$\theta = 5.0$$

$$\rho = 2.0$$

$$\kappa = ON * \theta$$

$$\lambda = ON * \rho$$

$$\delta = OFF * \theta$$

$$\nu = OFF * \rho$$

20 coupled ordinary differential equations

$$\frac{dc3}{dt} = c2 * \beta - c3 * \alpha$$

$$\frac{dc2}{dt} = c3 * \alpha + c1 * \beta 1 - c2 * (\beta + \alpha 1)$$

$$\frac{dc1}{dt} = c2 * \alpha 1 + o * \beta 2 + i * \mu - c1 * (\beta 1 + 2 * \alpha 2)$$

$$\frac{do}{dt} = c1 * \alpha 2 + i * \alpha i + on * \rho + b * OFF + nb * \nu - o * (\beta 2 + \beta i + \theta + ON + \kappa)$$

$$\frac{di}{dt} = c1 * \alpha 2 + o * \beta i - i * (\mu + \alpha i)$$

$$\frac{dcn3}{dt} = cn2 * \beta n - cn3 * \alpha n$$

$$\frac{dcn2}{dt} = cn3*\alpha n + cn1*\beta n1 - cn2*(\beta n + \alpha n1)$$
$$\frac{dcn1}{dt} = cn2*\alpha n1 + on*\beta n2 + in*\mu n - cn1*(\beta n1 + 2*\alpha n2)$$
$$\frac{don}{dt} = cn1*\alpha n2 + in*\alpha ni + o*\theta + b*\delta + nb*OFF - on*(\beta n2 + \beta ni + \rho + \lambda + ON)$$
$$\frac{din}{dt} = cn1*\alpha n2 + on*\beta ni - in*(\mu n + \alpha ni)$$
$$\frac{dcb3}{dt} = cb2*\beta - cb3*\alpha$$
$$\frac{dcb2}{dt} = cb3*\alpha + cb1*\beta 1 - cb2*(\beta + \alpha 1)$$
$$\frac{dcb1}{dt} = cb2*\alpha 1 + b*\beta 2 + ib*\mu - cb1*(\beta 1 + 2*\alpha 2)$$
$$\frac{db}{dt} = cb1*\alpha 2 + ib*\alpha i + o*ON + on*\lambda + nb*\rho - b*(\beta 2 + \beta i + OFF + \delta + \theta)$$
$$\frac{dib}{dt} = cb1*\alpha 2 + b*\beta i - ib*(\mu + \alpha i)$$
$$\frac{dcnb3}{dt} = cnb2*\beta n - cnb3*\alpha n$$
$$\frac{dcnb2}{dt} = cnb3*\alpha n + cnb1*\beta n1 - cnb2*(\beta n + \alpha n1)$$
$$\frac{dcnb1}{dt} = cnb2*\alpha n1 + nb*\beta n2 + inb*\mu n - cnb1*(\beta n1 + 2*\alpha n2)$$
$$\frac{dnb}{dt} = cnb1*\alpha n2 + inb*\alpha ni + o*\kappa + on*ON + b*\theta - nb*(\beta n2 + \beta ni + \nu + OFF + \rho)$$
$$\frac{dinb}{dt} = cnb1*\alpha n2 + nb*\beta ni - inb*(\mu n + \alpha ni)$$

Initial Conditions

$$c3 = \frac{\rho}{\rho + \theta} = 0.285714286$$
$$c2 = c1 = o = i = cb3 = cb2 = cb1 = b = ib = 0$$
$$cn3 = \frac{\theta}{\rho + \theta} = 0.714285714$$
$$cn2 = cn1 = on = in = cnb3 = cnb2 = cnb1 = nb = inb = 0$$

Calculation of Current

$\overline{G}_{hERG}$ = 0.0048 mS, Fink modified[3], ten Tusscher[4]

$\overline{G}_{hERG}$ = 0.015 mS, Priebe and Buekelmann[7]

$\overline{G}_{hERG}$ = 0.02614 mS, Luo and Rudy[8]

$$E_K = \frac{RT}{F}\ln\left(\left[K^+\right]_o / \left[K^+\right]_i\right)$$

$$I_{hERG,1a} = \overline{G}_{hERG} * \sqrt{\left[K^+\right]_o / 5.4} * (o + on) * (V - E_K)$$

1. Silva J, Rudy Y. Subunit interaction determines IKs participation in cardiac repolarization and repolarization reserve. *Circulation.* 2005;112:1384-1391.
2. Coleman TF, Li Y. *An Interior Trust Region Approach for Nonlinear Minimization Subject to Bounds*: Cornell University; 1993.
3. Fink M, Noble D, Virag L, et al. Contributions of HERG K+ current to repolarization of the human ventricular action potential. *Prog Biophys Mol Biol.* 2008;96:357-376.
4. ten Tusscher KH, Panfilov AV. Alternans and spiral breakup in a human ventricular tissue model. *Am J Physiol Heart Circ Physiol.* 2006;291:H1088-1100.
5. Rush S, Larsen H. A practical algorithm for solving dynamic membrane equations. *IEEE Trans Biomed Eng.* 1978;25:389-392.
6. Cohen SD, Hindmarsh AC. CVODE, a stiff/nonstiff ODE solver in C. *Comput Phys.* 1996;10:138-143.
7. Priebe L, Beuckelmann DJ. Simulation study of cellular electric properties in heart failure. *Circ Res.* 1998;82:1206-1223.
8. Faber GM, Rudy Y. Action potential and contractility changes in [Na(+)](i) overloaded cardiac myocytes: a simulation study. *Biophys J.* 2000;78:2392-2404.
9. Viswanathan PC, Rudy Y. Pause induced early afterdepolarizations in the long QT syndrome: a simulation study. *Cardiovasc Res.* 1999;42:530-542.
10. Zeng J, Rudy Y. Early afterdepolarizations in cardiac myocytes: mechanism and rate dependence. *Biophys J.* 1995;68:949-964.
11. Tan HL, Bardai A, Shimizu W, Moss AJ, Schulze-Bahr E, Noda T, Wilde AA. Genotype-specific onset of arrhythmias in congenital long-QT syndrome: possible therapy implications. *Circulation.* 2006;114:2096-2103.